

IDENTIFYING THE OUTFLOW DRIVING SOURCES IN ORION-KL

H. BEUTHER¹ & H.D. NISSEN²
beuther@mpia.de, hdn@phys.au.dk

Draft version from October 25, 2018, accepted for ApJL

ABSTRACT

The enigmatic outflows of the Orion-KL region have raised discussions about their potential driving sources for several decades. Here, we present C¹⁸O(2–1) observations combined from the Submillimeter Array and the IRAM 30m telescope. The molecular gas is associated on large scales with the famous northwest-southeast high-velocity outflow whereas the high-velocity gas on small spatial scales traces back to the recently identified submm source SMA1. Therefore, we infer that SMA1 may host the driving source of this outflow. Based on the previously published thermal and maser SiO data, source *I* is the prime candidate to drive the northeast-southwest low-velocity outflow. The source SMA1 is peculiar because it is only detected in several submm wavelength bands but neither in the infrared nor cm regime. We discuss that it may be a very young intermediate- to high-mass protostar. The estimated outflow masses are high whereas the dynamical time-scale of the outflow is short of the order 10³ yrs.

Subject headings: stars: formation – stars: early-type – stars: individual (Orion-KL) – ISM: jets and outflows

1. INTRODUCTION

The explosive large-scale northwest-southeast outflow in the Orion-KL region is one of the best studied but probably also least understood outflows in the sky. No other region shows that many H₂ bow shocks distributed in a fan-like fashion with red- and blue-shifted emission features on both sides of the central region (e.g., Schultz et al. 1999; Nissen et al. 2007). Furthermore, the molecular emission as traced in CO shows extremely broad line-wings up to > 50 km s⁻¹, but the morphological structure has so far been unclear and difficult to match closely to the H₂ outflow (e.g., Chernin & Wright 1996; Rodríguez-Franco et al. 1999). In addition to this outflow, also known as the high-velocity outflow, there exists a second outflow in the northeast-southwest direction which was first detected by H₂O maser emission and which is often labeled as the low-velocity outflow (e.g., Genzel et al. 1981; Genzel & Stutzki 1989).

The major question is which sources drive the different outflows. While originally the infrared source IRc2 was a suspect, it was soon realized that one of the prime powering sources of the region is the very close-by radio source *I* (Menten & Reid 1995). This source is the site of vibrationally excited SiO maser emission, and the orientation of these masers allowed different interpretations of the associated outflow direction. While early work favored source *I* to drive the large-scale northwest-southeast outflow (e.g., Wright et al. 1995; Greenhill et al. 1998), more recent work on the maser data indicates that it rather belongs to the low-velocity northeast-southwest outflow (Greenhill et al. 2003). The latter interpretation finds additional support in thermal SiO observations that show an elongated structure centered on source *I* with an orientation also in the northeast-southwest (Blake et al. 1996; Beuther et al. 2005, see also Fig. 1). Since thermal SiO emission is usually attributed to shocks within outflows

(e.g., Schilke et al. 1997), the combination of the thermal and maser SiO emission strongly favors source *I* as the driving source of the low-velocity northeast-southwest outflow. Source *n* has also been discussed as a possible driving source of the northeast-southwest low-velocity outflow. It shows an elongation along position angle 100–130° in the mid-infrared which could be due to a disk (Shuping et al. 2004; Greenhill et al. 2004), and a roughly perpendicular elongation in the radio at 8.4 GHz which may be caused by an outflow (Menten & Reid 1995). The relationship between sources *I* and *n* in driving the northeast-southwest outflow(s) is unknown (for a discussion see, e.g., Shuping et al. 2004; Nissen et al. 2007).

That leaves as an open question which source is the culprit for driving the large-scale high-velocity northwest-southeast outflow? Bally (2008) recently suggested that this outflow may be powered by the dynamical decay of a massive star system, but other scenarios are possible as well. Based on low-resolution data, de Vicente et al. (2002) proposed the existence of another luminous source approximately 2'' south of source *I*. This source was unambiguously identified in the first sub-arcsecond resolution 865 μm submm continuum image obtained with the Submillimeter Array (SMA), and henceforth labeled SMA1 (Beuther et al. 2004, see also Fig. 1). Follow-up SMA observations at 440 μm detected the source at these shorter wavelengths as well (Beuther et al. 2006). In this work we show that the high-velocity gas, as traced by C¹⁸O, apparently traces back to this relatively unknown source rather than to sources *I* or *n*.

2. OBSERVATIONS

Orion-KL was observed with the SMA in the compact configuration simultaneously at 690 GHz and 230 GHz on 2005 February 19th. To accomplish the high-frequency observations the weather conditions were excellent with zenith opacities $\tau(230\text{ GHz})$ between 0.03 and

¹ Max Planck Institute for Astronomy, Königstuhl 17, 69117 Heidelberg, Germany

² Department of Physics and Astronomy, University of Aarhus, 8000 Aarhus C, Denmark

0.04 throughout the night. The phase center was the nominal position of source *I* R.A.(J2000) 05h35m14.50s and decl.(J2000) 05°22'30."45, and the v_{LSR} was $\sim 5 \text{ km s}^{-1}$. The double-sideband receivers covered the frequency ranges 218.85 to 220.85 GHz and 228.85 to 230.85 GHz. The phase was calibrated with regularly interleaved observations of the quasar 0607-157, flux and bandpass calibration were performed with Callisto observations. The high-frequency data along with more observational details are published in Beuther et al. (2006), here we are only interested in a small subset of the low-frequency data. Complimentary $\text{C}^{18}\text{O}(2-1)$ data were obtained with the 9 pixel HERA array on the IRAM 30 m telescope in September 2007. The observations covered a region of $1' \times 1'$ around source *I* and were conducted in the on-the-fly mode with on-source integration times per position of ~ 3.7 secs. The OFF-source reference position was $15'$ east of source *I*. The single-dish data were converted to visibilities and subsequently processed with the SMA data within the MIRIAD package using standard tools (e.g., UVMODEL). The weighting of the two datasets was chosen to recover large-scale emission but maintain at the same time the high spatial resolution to resolve small-scale structure. The synthesized beam of the combined data is $4.2'' \times 3.3''$, and the 1σ rms per 5 km s^{-1} channel is $\sim 50 \text{ mJy beam}^{-1}$.

3. RESULTS

The whole low-frequency SMA dataset will be presented in a forthcoming publication by Nissen et al. (in prep.), here we are only interested in the $\text{C}^{18}\text{O}(2-1)$ emission. Although the SMA and IRAM 30 m observations also covered the more abundant isotopologues $^{12}\text{CO}(2-1)$ and $^{13}\text{CO}(2-1)$, in Orion-KL it turns out that because of their high optical depth these two lines strongly suffer from confusion problems with the ambient cloud complicating any interpretation of the data. In contrast to that, the rarer isotopologue $\text{C}^{18}\text{O}(2-1)$ penetrates the ambient cloud more deeply and hence traces the outflow associated gas far better, allowing us a deeper analysis of the outflow structure, its mass flow rate, kinematics and energetics, as well as pinpointing the likely driving source. Fig. 2 presents the combined SMA+30 m $\text{C}^{18}\text{O}(2-1)$ channel map. Excluding the channels with strongest emission closest to the v_{LSR} (approximately four channels between 0 and 15 km s^{-1}), two main features can be distinguished in the remaining channels:

(1) The large-scale gas emission exhibits a V-shaped cone-like open structure to the northwest, particularly prominent in the red-shifted channels $\geq 20 \text{ km s}^{-1}$ but also visible in the blue-shifted channels between -20 and -10 km s^{-1} . This cone-like structure approximately encompasses the main features of shocked strong H_2 emission in this direction (Fig. 3). Finding both blue- and red-shifted gas to the northwest indicates a wide opening angle of the flow where the main outflow axis is not too far from the plane of the sky. The less pronounced emission to the southeast was already previously observed, and Chernin & Wright (1996) argue that the outflow may be blocked in this direction by the hot core³. It is interesting to note that the main southeastern emission features are

well correlated with a lack of H_2 emission indicating particularly high column densities in this direction. Furthermore, we find high-velocity gas toward the southwest and northeast (Fig. 3). Since Nissen et al. (2007) find H_2 emission with velocities up to 40 km s^{-1} toward the southwest as well, it is likely that this high-velocity gas is associated with the low-velocity outflow.

(2) We find that the high-velocity gas on the blue- and red-shifted side of the spectrum traces back to the source SMA1. Although the synthesized beam is larger than the spatial separation of source *I* and SMA1 ($\sim 2''$ or $\sim 830 \text{ AU}$), the peak positions can be determined with a much higher spatial accuracy depending on the signal-to-noise ratio S/N. For point sources, one can in principle achieve an accuracy of $0.45 \text{ HPBW}/(\text{S/N})$ (Reid et al. 1988), however, this may be less applicable for extended emission like C^{18}O in this case. The channel with the lowest S/N ratio still detects the main peak position toward SMA1 at higher than 15σ values (at -30 km s^{-1}). For a point source, this would imply that the peak positions could be determined to better than $0.125''$. Although the C^{18}O emission is more extended, the shape of the high-velocity gas close to SMA1 can to first order be described by a two-dimensional Gaussian. Therefore, being more conservative for the C^{18}O high-velocity gas, it should still be possible to infer the emission peak positions to an accuracy of better than $1''$. Based on this, the blue- and red-shifted high-velocity gas is spatially mainly associated with SMA1, and not with the previously often discussed sources *I* or *n*.

The blue- and red-shifted maps shown in Figure 3 (integrated from -35 to -20 and from 22.5 to 37.5 km s^{-1} , respectively) can be used to calculate the masses, kinematic and energetic parameters of the outflow following Beuther et al. (2002b) (time-scale t , outflow rate \dot{M}_{out} , momentum rate p , and energy E). Assuming optically thin $\text{C}^{18}\text{O}(2-1)$ emission at 30 K with a $\text{C}^{18}\text{O}/\text{H}_2$ conversion factor of 1.7×10^{-7} (Frerking et al. 1982), the derived values are given in Table 1. While the masses have uncertainties of approximately a factor 5, the kinematic and energetic values are uncertain within an order of magnitude (Cabrit & Bertout 1990). The derived masses, outflow and momentum rates are at the upper end of typically found massive outflows, whereas the time-scale is relatively short (compared with the outflow sample in Beuther et al. 2002b).

4. DISCUSSION AND CONCLUSIONS

The large-scale cone-like morphology of the C^{18}O outflow approximately following the H_2 bow-shock emission in the northwest direction suggests that C^{18}O and H_2 are tracing the same outflow. Furthermore, the spatial association of the C^{18}O high-velocity emission with the submm source SMA1 indicates that SMA1 may harbor the driving source of the enigmatic large-scale Orion-KL outflow. Only the combination of the single-dish 30 m data, tracing the large-scale structure, with the SMA high-spatial-resolution observations allows us to see all relevant structures and to trace the outflow back to pinpoint its origin.

³ The hot core traced in NH_3 (Wilson et al. 2000) actually extends further southeast of SMA1 than indicated by the hot core continuum peak in Fig. 1. The proposed blocking of the outflow by the hot core may also be responsible for some of the large-scale asymmetries of the H_2 emission.

In combination with the thermal and maser SiO data, we suggest that the two driving sources of the two known outflows can be identified: (1) SMA1 may host the driving source of the large-scale northwest-southeast high-velocity outflow, whereas (2) source *I* is likely the origin of the northeast-southwest low-velocity outflow.

The nature of source *I* has been subject to many investigations for more than a decade (e.g., Menten & Reid 1995; Beuther et al. 2006; Reid et al. 2007), however, we do not know much about SMA1. So far SMA1 has only been detected at submm wavelengths (865 and 440 μm , Beuther et al. 2004, 2006) but neither at shorter infrared nor at longer cm wavelengths (e.g., Menten & Reid 1995; Greenhill et al. 2004). The submm-only detection is indicative of a very young age of the source which is supported by the short dynamical time-scale of the molecular outflow. Although deriving a luminosity with just two data-points is impossible, based on the large outflow masses, it is likely that SMA1 is in the process of forming a massive star. The non-detection at cm wavelengths could either be due to quenching of an underlying hypercompact HII region by very high accretion rates and/or gravitational trapping of the ionized gas (e.g., Walmsley 1995; Keto 2003), or the source is still in such a young evolutionary phase that the central object has not yet enough ionizing flux to produce a detectable hypercompact HII region. In the framework of the recently proposed evolutionary sequence by Beuther et al. (2007), it may be an intermediate-mass protostar destined to become massive in the future.

Assuming optically thin dust emission at 100 K with a dust opacity index $\beta = 2$ (e.g., Hildebrand 1983; Beuther et al. 2002a), the spatially resolved submm fluxes (Beuther et al. 2004, 2006) correspond to a gas mass and

column density of $\sim 0.1 M_{\odot}$ and 3×10^{24} , respectively. While the large column densities confirm that this source is undetectable at near-infrared wavelengths with current instrumentation, at first sight the mass appears small. However, as discussed in (Beuther et al. 2004), more than 90% of the total flux is filtered out by the SMA observations, and hence the mass estimates are correspondingly unreliable. The total luminosity of the region of about $10^5 L_{\odot}$ (e.g., Menten & Reid 1995) cannot be produced by the sources previously discussed in the literature (e.g., Greenhill et al. 2004), and it is well possible that SMA1 contributes a significant fraction of the overall Orion-KL luminosity.

We note that the short dynamical outflow time-scale of the order 10^3 yrs is consistent with both recently discussed scenarios for the proper motions in this region: Tan (2005) proposed that the recent passage of the BN-object has triggered the outflow burst in this region, whereas Rodríguez et al. (2005) and Gómez et al. (2005) suggest that a dynamically decaying multiple system is at the root of the observed proper motions. Both events are suggested to have taken place about 500 yrs ago. Our data do not allow to differentiate between these scenarios, however, it is interesting that all recent observations are indicative of strong activity within the last 10^3 yrs.

H.B. acknowledges financial support by the Emmy-Noether-Programm of the Deutsche Forschungsgemeinschaft (DFG, grant BE2578). H.D.N. acknowledges the support of the Aarhus Centre for Atomic Physics (ACAP), funded by the Danish Basic Research Foundation and the financial support from the Instrument Centre for Danish Astrophysics (IDA), funded by the Danish National Science Committee (FNU).

REFERENCES

- Bally, J. 2008, ASP Conference Series 387, Proceedings to conference "The Formation of Massive Stars: Observations Confront Theory", astro-ph/0712.1997
- Beuther, H., Churchwell, E. B., McKee, C. F., & Tan, J. C. 2007, in Protostars and Planets V, ed. B. Reipurth, D. Jewitt, & K. Keil, 165–180
- Beuther, H., Schilke, P., Menten, K. M., et al. 2002a, ApJ, 566, 945
- Beuther, H., Schilke, P., Sridharan, T. K., et al. 2002b, A&A, 383, 892
- Beuther, H., Zhang, Q., Greenhill, L. J., et al. 2004, ApJ, 616, L31
- . 2005, ApJ, 632, 355
- Beuther, H., Zhang, Q., Reid, M. J., et al. 2006, ApJ, 636, 323
- Blake, G. A., Mundy, L. G., Carlstrom, J. E., et al. 1996, ApJ, 472, L49
- Cabrit, S. & Bertout, C. 1990, ApJ, 348, 530
- Chernin, L. M. & Wright, M. C. H. 1996, ApJ, 467, 676
- de Vicente, P., Martín-Pintado, J., Neri, R., & Rodríguez-Franco, A. 2002, ApJ, 574, L163
- Frerking, M. A., Langer, W. D., & Wilson, R. W. 1982, ApJ, 262, 590
- Genzel, R., Reid, M. J., Moran, J. M., & Downes, D. 1981, ApJ, 244, 884
- Genzel, R. & Stutzki, J. 1989, ARA&A, 27, 41
- Gómez, L., Rodríguez, L. F., Loinard, L., et al. 2005, ApJ, 635, 1166
- Greenhill, L. J., Chandler, C. J., Reid, M. J., et al. 2003, in IAU Symposium
- Greenhill, L. J., Gezari, D. Y., Danchi, W. C., et al. 2004, ApJ, 605, L57
- Greenhill, L. J., Gwinn, C. R., Schwartz, C., Moran, J. M., & Diamond, P. J. 1998, Nature, 396, 650
- Hildebrand, R. H. 1983, QJRAS, 24, 267
- Keto, E. 2003, ApJ, 599, 1196
- Menten, K. M. & Reid, M. J. 1995, ApJ, 445, L157
- Nissen, H. D., Gustafsson, M., Lemaire, J. L., et al. 2007, A&A, 466, 949
- Reid, M. J., Menten, K. M., Greenhill, L. J., & Chandler, C. J. 2007, ApJ, 664, 950
- Reid, M. J., Schneps, M. H., Moran, J. M., et al. 1988, ApJ, 330, 809
- Rodríguez, L. F., Garay, G., Brooks, K. J., & Mardones, D. 2005, ApJ, 626, 953
- Rodríguez-Franco, A., Martín-Pintado, J., & Wilson, T. L. 1999, A&A, 351, 1103
- Schilke, P., Walmsley, C. M., Pineau des Forets, G., & Flower, D. R. 1997, A&A, 321, 293
- Schultz, A. S. B., Colgan, S. W. J., Erickson, E. F., et al. 1999, ApJ, 511, 282
- Shuping, R. Y., Morris, M., & Bally, J. 2004, AJ, 128, 363
- Tan, J. C. 2005, in IAU Symposium, ed. R. Cesaroni, M. Felli, E. Churchwell, & M. Walmsley, 318–327
- Walmsley, M. 1995, in Revista Mexicana de Astronomia y Astrofisica Conference Series, 137
- Wilson, T. L., Gaume, R. A., Gensheimer, P., & Johnston, K. J. 2000, ApJ, 538, 665
- Wright, M. C. H., Plambeck, R. L., Mundy, L. G., & Looney, L. W. 1995, ApJ, 455, L185

TABLE 1
OUTFLOW PARAMETER

$M_{\text{blue}} [M_{\odot}]$	33
$M_{\text{red}} [M_{\odot}]$	81
$M_{\text{total}} [M_{\odot}]$	124
$t [\text{yr}]$	971
$\dot{M}_{\text{out}} [M_{\odot} \text{ yr}^{-1}]$	1.2×10^{-1}
$p [M_{\odot} \text{ km s}^{-1}]$	3980
$E [\text{erg}]$	1.4×10^{48}

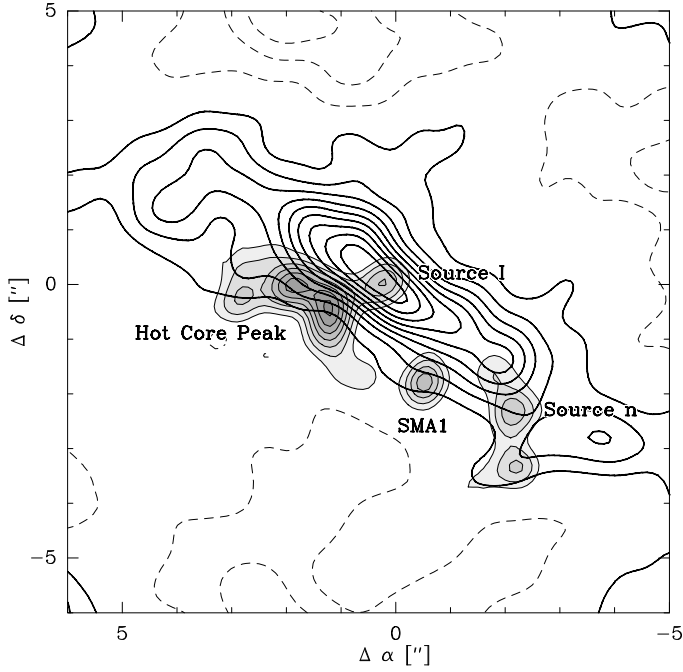


FIG. 1.— SiO(8–7) integrated emission as contour overlay on the grey-scale $865\ \mu\text{m}$ submm continuum emission obtained with the SMA. This figure is an adaption of the $865\ \mu\text{m}$ continuum and SiO(8–7) line data from Beuther et al. (2004, 2005). The grey-scale continuum contours start at the 3σ level of $0.105\ \text{mJy beam}^{-1}$ and continues in 2σ steps. The SiO emission is contoured from ± 10 to $\pm 90\%$ (step $\pm 10\%$) of the peak emission of $2.1\ \text{Jy beam}^{-1}$ with full and dashed contours as positive and negative features (due to missing short spacings), respectively.

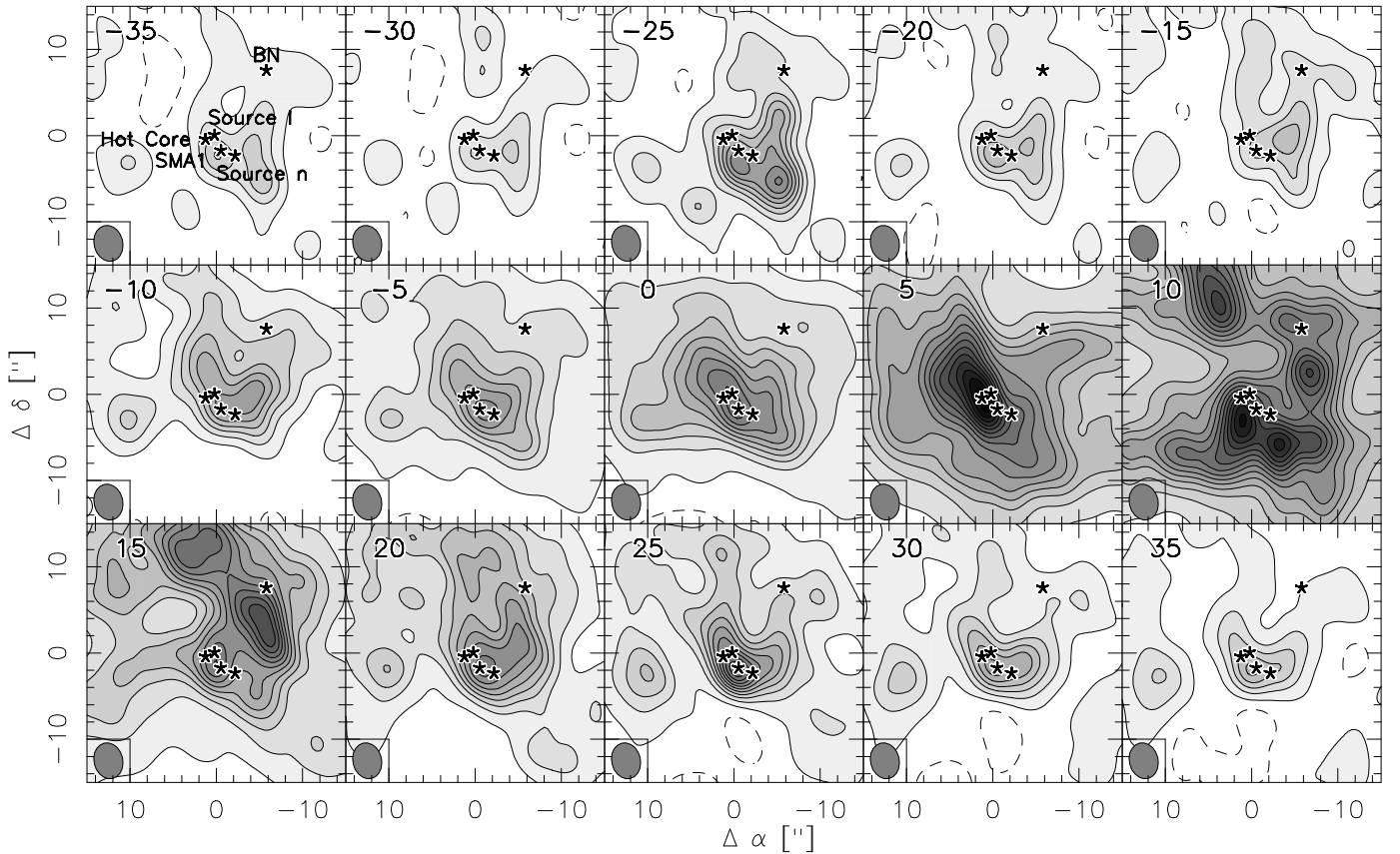


FIG. 2.— $\text{C}^{18}\text{O}(2-1)$ channel map with $5\ \text{km s}^{-1}$ of the combined SMA+30m data. The contours start at the 3σ levels of $150\ \text{mJy beam}^{-1}$ and continue in 6σ steps for all panels except of the 0, 5 and $10\ \text{km s}^{-1}$ panels that follow 12, 12 and 14σ steps for clarity reasons. Negative features are drawn as dashed contours. The stars mark the positions of the five main continuum source with labels in the top-left panel. The synthesized beam is shown at the bottom-left of each panel.

FIG. 3.— Overlay of the H_2 emission in grey-scale (Nissen et al. 2007) with the blue- and red-shifted $\text{C}^{18}\text{O}(2-1)$ emission in color-contours. The integration ranges are $[-35.0/-20.0]$ and $[22.5,37.5]$ km s^{-1} , respectively. The contours are in 3σ steps of $150 \text{ mJy beam}^{-1}$. The stars mark the positions of the same continuum sources as in Figure 2, the synthesized beam is shown at the top-right of each panel. The large circle in the left panel shows the size of the SMA primary beam, whereas the squared box marks the size of the inlay-box shown in the right panel. The outflow directions of the high- and low-velocity outflow are sketched in the left panel.

This figure "f3.jpg" is available in "jpg" format from:

<http://arxiv.org/ps/0804.2539v1>